J. Phys. F: Met. Phys. **18** (1988) 833–849. Printed in the UK

First-principles calculations of the optical properties of metals

E G Maksimov, I I Mazin, S N Rashkeev and Yu A Uspenski
P N Lebedev Physical Institute, Leninski 53, 117924 Moscow, USSR

Received 8 April 1987, in final form 8 July 1987

Abstract. We have calculated the optical properties (dielectric function, reflectivity and electron energy loss function) of 15 metals, including all the 4d series, some 3d metals and some noble and simple metals. The calculations are based on the LMTO band structure with optical matrix elements. The very good quantitative agreement with optical measurements provides an *a posteriori* justification of the use of local density functional method in the calculations of the dynamical response in metals and also allows an analysis of the general trends in optical properties from the electronic structure point of view.

1. Introduction

It is well known that optical experiments provide a considerable amount of varied information about the band structure of metals and the collective excitations in them. Such information is extremely valuable for metal physicists, to say nothing of its great practical importance in metal optics. However, it is not a trivial task to extract this information from experimental data. In simple metals one has a good theoretical basis for the interpretation of measurements, namely the homogeneous electron gas model and the theory of pseudopotentials. A complete description of the problems concerning simple metals may be found in the reviews by Motulevich (1969) and Sturm (1982) and in the book by Pines (1963).

The case of transition metals is much more complicated. Only a very limited amount of information may be extracted from experiments because of the lack of an appropriate theoretical basis. Recently some authors have used the density functional method combined with the random phase approximation (RPA) for direct calculation of the optical properties of metals. It is nearly impossible to estimate *a priori* the validity of these approximations. However, there is empirical evidence that in simple metals and transition metals the density functional band structure is very close to the excitation spectrum. Our systematic study of the optical properties of 4d and other transition metals has given results (which are the subject of this paper) very close to the experimental results.

In this paper, which summarises the results of our recent investigations (1983–6), we present detailed calculations of the optical properties (dielectric function, optical conductivity and electron energy loss function) of 15 metals, including all the 4d metals, in an energy range up to 35 eV, based on LMTO band structure calculations. In spite of neglecting all effects beyond the RPA, as well as local field and finite lifetime

0305-4608/88/040833 + 17 $02.50

effects in interband transitions, we find a very good agreement between the calculations and experiments. This allows us to estimate the validity of the approximations and to analyse the microscopical nature of the optical spectra of the metals investigated.

The paper is organised as follows. In § 2 we recall the necessary formulae, describe the calculational technique and discuss the accuracy of the calculations. In § 3 we present the results of the calculations and discuss them. Our conclusions are summarised in § 4.

2. Calculational technique and approximations

The optical properties of matter are determined by the macroscopical dielectric function $\varepsilon_M(\omega) = \varepsilon_M(\omega, \boldsymbol{q} \to 0)$. We deal in this paper only with cubic crystals where we can consider the dielectric function (DF) as a scalar and need not distinguish between the transverse and longitudinal DF.

The following approximate formula for $\varepsilon_M(\omega, \boldsymbol{q})$ is widely used:

$$\varepsilon_M(\omega, \boldsymbol{q}) = 1 + \frac{8\pi e^2}{\Omega q^2} \sum_{k,\lambda,\lambda'} \frac{|\langle \boldsymbol{k}+\boldsymbol{q}, \lambda' | e^{i\boldsymbol{q}\cdot\boldsymbol{r}} | \boldsymbol{k}\lambda \rangle|^2 (f_{k\lambda} - f_{k+q,\lambda'})}{E_{k\lambda} - E_{k+q,\lambda'} + \hbar\omega + i\delta} \tag{1}$$

where $|\boldsymbol{k}\lambda\rangle$ is the Bloch wavefunction of the electron in the band λ with wavevector $\boldsymbol{k}$ and energy $E_{k\lambda}$, and $f_{k\lambda}$ is the Fermi distribution function, all the quantities being calculated from the Kohn–Sham equations of the density functional theory (DFT).

The validity of this approach may be argued in two ways. Firstly, equation (1) may be considered as an RPA formula without the local field corrections where the one-electron Green function is approximated by that of the Kohn–Sham equations. As the latter have real eigenvalues $E_{k\lambda}$, the lifetime of the one-electron excitation is inifinite in this model. In fact, there is always a decay of these excitations due to many-electron effects, which is stronger the further the energy in question is from the Fermi level. Moreover, the Kohn–Sham $E_{k\lambda}$ may differ from the actual one-electron excitation energies, again by a greater amount the greater $|E_{k\lambda} - E_F|$ is. Both effects lead to the smoothing and sometimes to the distortion of the optical spectra at high frequencies. Fortunately, in simple metals and transition metals (but not in insulators) these effects are small enough in a sufficiently large energy region ($|E_{k\lambda} - E_F| \lesssim \hbar\omega_p$).

An alternative approach is that due to the generalisation of the DFT to the time-dependent external fields (Runge and Gross 1984). Indeed, if we assume that the DFT exchange correlation potential changes in a weak external potential $\delta V_{ext}(\boldsymbol{r}, t)$ only as a result of the change in the density, then

$$\left(-\frac{\hbar^2\nabla^2}{2m} + V_{eff}(n(\boldsymbol{r}) + \delta n(\boldsymbol{r}, t)) + \delta V_{ext}(\boldsymbol{r}, t) \right) \varphi_k(\boldsymbol{r}, t) = i\hbar \frac{\partial}{\partial t} \varphi_k(\boldsymbol{r}, t) \tag{2}$$

where the density is defined by the wavefunctions $\varphi_k(\boldsymbol{r}, t)$ in the usual Kohn–Sham manner. One may expect this approach to yield reasonable results for sufficiently low frequencies. Indeed, the calculation of the photoabsorption of rare-gas atoms, carried out using equation (2), turned out to be quite accurate (Zangwill and Soven 1980). Equation (2) includes the local field corrections as well as the ladder diagrams with $I_{xc}(\boldsymbol{r}, \boldsymbol{r}') = \delta V_{xc}(\boldsymbol{r})/\delta n(\boldsymbol{r}')$ and therefore goes beyond the RPA. Neither this latter effect nor the local field correction is included in equation (1), which may be considered as a

further approximation to equation (2). The local field effects arise because of the fact that the macroscopical DF is determined by the inverse microscopical dielectric matrix:

$$\varepsilon_M(\omega,\ \boldsymbol{q}) = 1/\varepsilon^{-1}(\omega,\ \boldsymbol{q}+\boldsymbol{G},\ \boldsymbol{q}+\boldsymbol{G}')|_{G=G'=0}. \tag{3}$$

For $\boldsymbol{q}\rightarrow 0$, neglecting both effects not included in (1) is partly justified; it can be shown (Singhal 1976, Mazin *et al* 1986) that there is strong compensation because only the sum of these two (nearly equal in magnitude and opposite in sign) expressions enters the equations, i.e.

$$[I_{xc}(\boldsymbol{q}+\boldsymbol{G}, \boldsymbol{q}+\boldsymbol{G}') + \delta_{GG'}(4\pi e^2/|\boldsymbol{q}+\boldsymbol{G}|^2)]_{G,G'\neq 0}.$$

Neglecting one of these effects is thus likely to be worse than neglecting both.

Using the continuity equation, equation (1) may be rewritten for $\boldsymbol{q}\rightarrow 0$ as

$$\varepsilon_M(\omega) = \varepsilon^{\text{intra}}(\omega) + \frac{8\pi e^2\hbar^2}{3m^2(2\pi)^3}\int \mathrm{d}\boldsymbol{k} \sum_{\lambda\neq\lambda'} \frac{2f_{k\lambda}(1-f_{k\lambda'})|P^{\boldsymbol{k}}_{\lambda\lambda'}|^2}{(E_{k\lambda'}-E_{k\lambda})[(E_{k\lambda'}-E_{k\lambda})^2-(\hbar\omega)^2-\mathrm{i}\delta]} \tag{4}$$

where we have divided $\varepsilon_M(\omega)$ into the intraband and interband contributions and $\boldsymbol{p}^{\boldsymbol{k}}_{\lambda\lambda'} = \langle \boldsymbol{k}\lambda|\hbar\nabla/\mathrm{i}|\boldsymbol{k}\lambda'\rangle$ is the moment matrix element. For the intraband DF we have used the Drude formula

$$\varepsilon^{\text{intra}}(\omega) = 1 - \bar{\omega}_p^2/\omega(\omega+\mathrm{i}\gamma) \tag{5}$$

where γ is the relaxation frequency and $\bar{\omega}_p^2$ is given by

$$\bar{\omega}_p^2 = \frac{8\pi e^2}{3\Omega}\sum_{\lambda,\boldsymbol{k}} |\boldsymbol{V}_{k\lambda}|^2\delta(E_{k\lambda}-E_F), \tag{6}$$

with

$$\boldsymbol{V}_{k\lambda} = \frac{1}{m}\boldsymbol{P}^{\boldsymbol{k}}_{\lambda\lambda} = \frac{1}{\hbar}\frac{\partial E_{k\lambda}}{\partial \boldsymbol{k}} \tag{7}$$

the velocity of the electron in the state $|\boldsymbol{k}\lambda\rangle$.

The scheme for our calculations of the optical properties was as follows. The interband part of $\varepsilon_2(\omega)$ was calculated from equation (4). The self-consistent band structure and the wavefunctions have been computed by the LMTO method (Andersen 1975) with $l_{max}=3$. The matrix elements of the interband transitions have been calculated as described by Uspenskii *et al* (1983). The accuracy of the calculated matrix elements has been tested by checking the fulfilment of the exact equality (7). The reciprocal space integration has been performed by means of the tetrahedron method, usually with 204 and 175 points in the irreducible part of the Brillouin zone for BCC and FCC metals respectively†. The real part $\varepsilon_1(\omega)$ has been obtained from the Kramers–Kronig relation. The numerical integration over ω has been performed with a step of 0.01 Ryd, the upper limit $\hbar\omega_{max}\sim 5$ Ryd being chosen to cover all non-zero $\varepsilon_2^{\text{inter}}(\omega)$. The total error of integration in the Kramers–Kronig transformation is estimated as 0.5%.

The parameters of the intraband part of the DF, $\bar{\omega}_p$ and γ, have also been calculated *ab initio* using the method described by Mazin *et al* (1984). Then we have

† It should be noted that there are cases where these numbers of points are insufficient to obtain some details of the optical spectra correctly. One such case is Al which is described below. Another example is our investigation of infrared absorption in transition metals (Rashkeev *et al* 1985), for which we had to use as many as 4000 points.

computed the reflectivity $R(\omega)$ and the energy loss function $L(\omega)$ using the total DF, $\varepsilon(\omega)$.

Now we turn to a short discussion of the accuracy of the calculations. It is well known that the error in LMTO calculations of band structures is some 0.1 eV for the energy region $\hbar\omega \leqslant 15$ eV. Our experience shows that for higher energies ($15 \leqslant \hbar\omega \leqslant 35$ eV) the LMTO method gives dispersion curves of the correct shape but raised by ~ 1 eV. For even higher energies ($\hbar\omega > 35$ eV) the calculated dispersion may be incorrect even qualitatively. The corresponding errors in the calculation of the matrix elements are $\leqslant 10\%$ for $\hbar\omega \leqslant 15$ eV, 20–40% for $15 \leqslant \hbar\omega \leqslant 35$ eV and as much as 50–100% for $\hbar\omega > 35$ eV.

In spite of this, we did include the region $\hbar\omega > 35$ eV in our calculations, bearing in mind that our $\varepsilon_2(\omega)$ for such high energies can be considered only as an extrapolation of the actual $\varepsilon_2(\omega)$ which is useful for the more accurate calculation of $\varepsilon_1(\omega)$ from the Kramers–Kronig relation. It may be noted that for a more open BCC lattice the error in the calculation of E_{kl} by the LMTO method (Andersen 1975) is greater than that for a FCC lattice. Therefore we expect a greater error in $\varepsilon_2(\omega)$ for the BCC metals than for the FCC ones. Another source of error is the neglect of core–valence transitions. The main effect of all these inaccuracies is the underestimation of $\varepsilon_1(\omega)$ by 0.1–0.3. This is relatively small and does not have much influence on $R(\omega)$ or $L(\omega)$ at $\hbar\omega \leqslant 35$ eV†.

An important integral characteristic of the DF is the energy-dependent effective number of electrons

$$N_{\text{eff}}(E) = \left(\frac{2\pi^2 e^2}{m\Omega}\right)^{-1} \int_0^{E/\hbar} \omega\varepsilon_2(\omega)\ \mathrm{d}\omega. \tag{8}$$

According to the well known f-sum rule, $N_{\text{eff}}(E \to \infty) = N_{\text{tot}}$, where N_{tot} is the total number of electrons per atom including all the core electrons. It is often useful to introduce the effective number of valence electrons, i.e. the contribution in (8) from the valence electron excitation. It is known (e.g. Wooten 1972) that $N_{\text{eff}}^{\text{val}}(E \to \infty)$ is greater than the actual number of valence electrons by the number of electrons corresponding to Pauli forbidden transitions between the core state and the occupied part of the valence band. In calculations $N_{\text{eff}}^{\text{val}}$ is underestimated because only a finite number of empty bands may be taken into account in the calculation of ε_2; therefore the calculated $N_{\text{eff}}^{\text{val}}$ may be either greater or less than N_{val}. Actually $N_{\text{eff}}^{\text{val}}$ is quite close to N_{val} (figure 1). In the discussion of our results we shall also use the effective number of electrons involved in a particular group of transitions (i.e. oscillator strength), defined as the contribution to (8) from the transitions in question.

3. Numerical results and comparison with experiments

We present here the calculations of the optical properties of 15 metals, among them a simple metal (Al), all the 4d transition metals, two 3d metals, (V, Cr), two noble metals (Cu, Ag) and two post-noble (Zn, Cd) metals. In order to investigate the general trends of the principle features of the optical spectra (including EELS), we included also some HCP metals (Y, Zr, Tc, Rn, Zn, Cd), which we have, however, treated as cubic. Such a treatment is undoubtedly inappropriate in describing the fine structure of the optical spectra, but gives a reasonable description of the large-scale

† In some previous publications (Mazin *et al* 1986, Rashkeev *et al* 1985) there was a numerical error in calculations of $\varepsilon_2^{\text{inter}}(\omega)$ that led to $\varepsilon_2^{\text{inter}}(\omega)$ being incorrect by a factor of $\pi/2$. This error worsened the agreement with experiment but did not influence the qualitative conclusions of those papers.

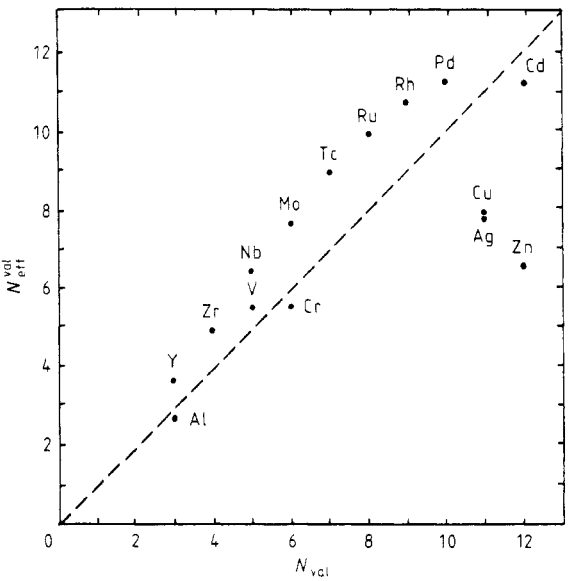

Figure 1. The fulfilment of the valence f-sum rule. The broken line corresponds to the ideal fulfilment $N_{\text{eff}}^{\text{val}} = N_{\text{val}}$.

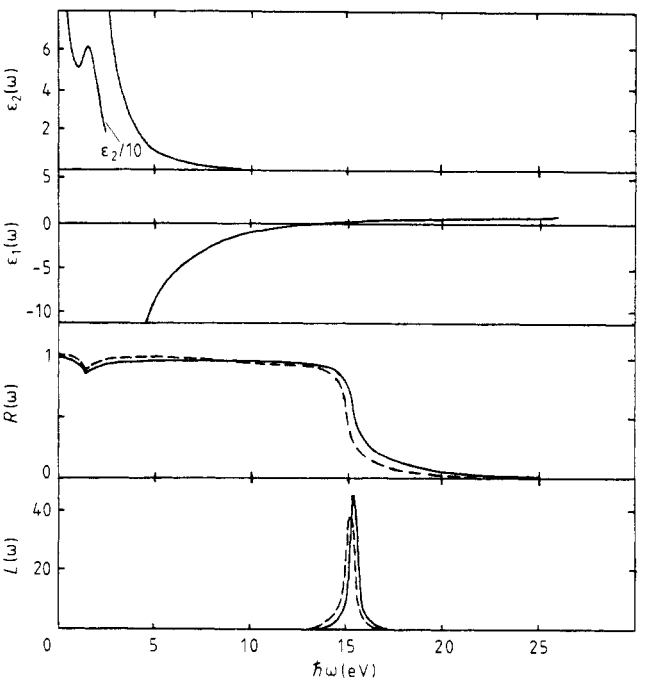

Figure 2. Optical properties of aluminium: full curves, calculations; broken curves, measurements of $R(\omega)$ and $L(\omega) = \text{Im}(-1/\varepsilon(\omega))$ (from Shiles *et al* 1980) (arbitrary units).

features defined mainly by the widths of the bands and their relative positions. The comparison with experiment confirms this.

Now we turn to the discussion of the particular groups of metals. In Al (a simple metal) an interband absorption edge lies near 0.5 eV (figure 2). At 1.6 eV $\varepsilon_2(\omega)$ has a strong maximum (corresponding to the gap at the (200) face of the Brillouin zone) and a smaller one at 0.8 eV. These give rise to a sharp minimum and a subtle feature, respectively, in $R(\omega)$. The EELS $L(\omega) = -\mathrm{Im}(1/\varepsilon(\omega))$ has a strong plasmon peak at 15.4 eV and a barely noticeable plasmon peak at 0.75 eV. The plasmon absorption edge at ~ 15.4 eV is clearly seen in $R(\omega)$. It is interesting that the subtle feature appearing at 0.8 eV in $\varepsilon_2(\omega)$ and $R(\omega)$ and at 0.75 eV in $L(\omega)$, which is hardly noticeable in the experimental curves and difficult to obtain theoretically (we need to include up to 4000 points in the 1/48 part of the Brillouin zone to catch it), is, however, quite important, because it increases rapidly with pressure. This increase has been established both experimentally† (Tups and Syassen 1984) and theoretically (Rashkeev and Halilov 1987).

The optical spectra of the transition metals are more complicated. Typical of this group are the spectra of FCC metals Rh and Pd (figures 3 and 4). $R(\omega)$ and $L(\omega)$ here have a number of minima and maxima, which are surprisingly well reproduced in the calculations. The BCC metals, being less packed than the FCC ones, are more difficult to deal with by the LMTO method. Indeed, in the energy range $\hbar\omega \leqslant 10$ eV the agreement is good (figures 5 and 6) but for higher energies it gets worse. The main reason is that the hybridized p–f band which lies some 10 eV higher than E_F is moved up in our calculations by about 1 eV (this is peculiar to the LMTO method). Therefore the increase of $\varepsilon_2(\omega)$ in Nb due to the optical transitions from the d band to the p–f band takes place not at 11 eV as the experiment shows but at 12 eV. For the same reason the broad minimum of $\varepsilon_2(\omega)$ at 10–11 eV becomes deeper, which leads to an unrealistic increase of the reflectivity in this region.

Thus we see that in cubic 4d metals at $\hbar\omega \leqslant 10$ eV the positions of the main features, as well as their magnitudes, are in good agreement with experiment. We may conclude that in this energy range the Kohn–Sham states closely approximate the one-electron excitations. Even at higher energies the discrepancies seem to be mainly due to the inaccuracies of the band structure calculations. However, there is evident manifestation of many-electron effects in the smoothing of the experimental curves, especially in $L(\omega)$. It has been shown (Zharnikov and Rashkeev 1984) that this cannot be explained solely by the insufficient experimental resolution, but must also be due to the finite lifetime of the electron excitations.

In 4d HCP metals (Y, Zr, Tc, Ru) we find reasonable agreement with experiment for $L(\omega)$ (figures 7–10). This means that the EELS are insensitive to the crystal structure (all HCP metals were treated as FCC). Indeed, we have done the calculation for a particular metal (Tc) also in the BCC lattice and found that the EELS was almost unaffected. For the reflectivity $R(\omega)$, only the general shapes of the curves are reproduced in our calculations, since the detailed structure of $R(\omega)$ is dependent on the crystal lattice.

For the 3d metals V and Cr the experimental data are relatively limited. In general the agreement between the measurements and the calculations is satisfactory (figures 11 and 12), though it seems worse than in the 4d metals. In principle this may be

† In all theoretical calculations at $P = 0$ (Alouani and Khan 1986, Rashkeev and Halilov 1987), including the present one, the maximum in $\varepsilon_2(\omega)$ is found to be 0.2 eV higher than in the measurements. This discrepancy persists at high pressures.

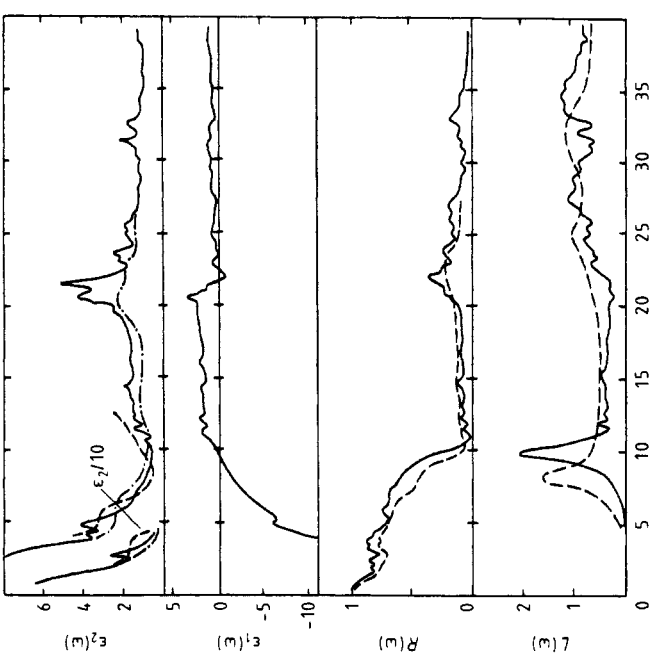

Figure 3. Optical properties of rhodium: full curves, calculations; broken curves, measurements of $\varepsilon_2(\omega)$ (from Pierce and Spicer 1973), $R(\omega)$ (from Seignac and Robin 1970) and $L(\omega)$ (from Lynch and Swan 1968); chain curve, measurements of $\varepsilon_2(\omega)$ (from Seignac and Robin 1970) (arbitrary units).

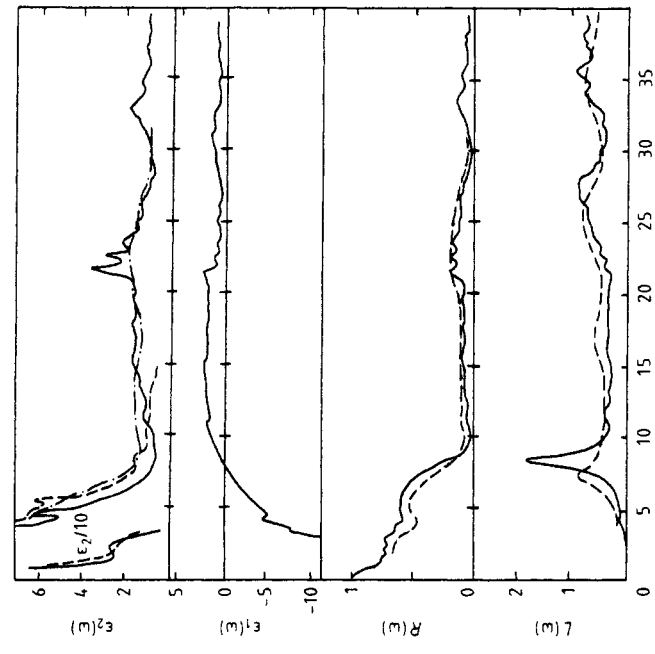

Figure 4. Optical properties of palladium: full curves, calculations; broken curves, measurements of $\varepsilon_2(\omega)$ (from Weaver 1973), $R(\omega)$ (from Vehse *et al* 1970) and $L(\omega)$ (from Daniels 1969); chain curve, measurements of $\varepsilon_2(\omega)$ (from Vehse *et al* 1970) (arbitrary units).

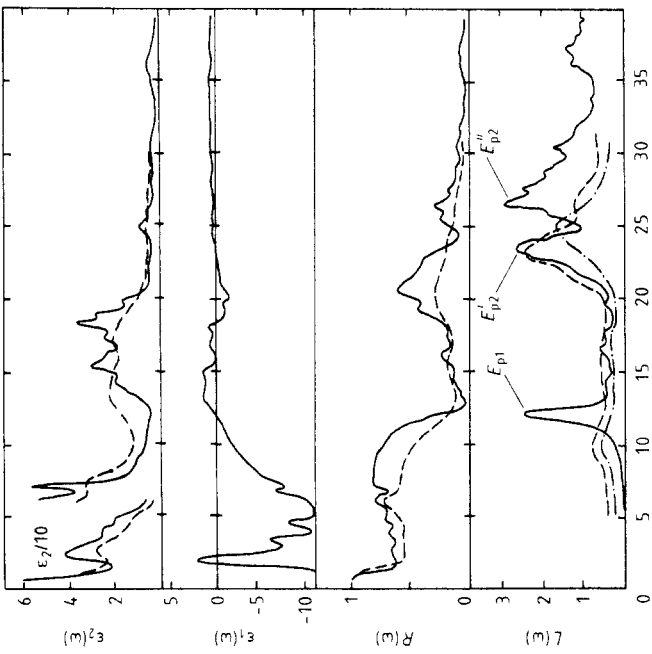

Figure 6. Optical properties of molybdenum: full curves, calculations; broken curves, measurements (from Mayevskii *et al* 1981); chain curve, measurements of $L(\omega)$ (from Weaver *et al* 1974) (arbitrary units).

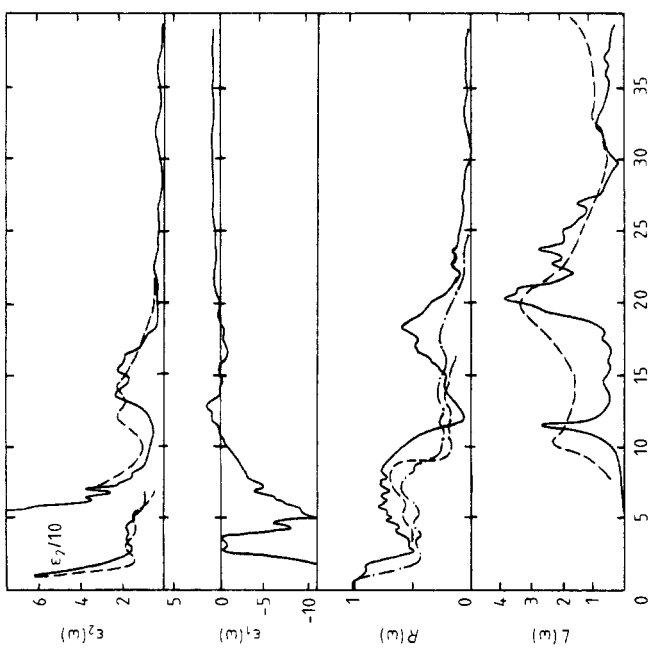

Figure 5. Optical properties of niobium: full curves, calculations; broken curves, measurements of $\varepsilon_2(\omega)$ (from Weaver *et al* 1973), $R(\omega)$ (from Vilesov *et al* 1967) and $L(\omega)$ (from Lynch and Swan 1968); chain curve, measurements of $R(\omega)$ (from Weaver *et al* 1973) (arbitrary units).

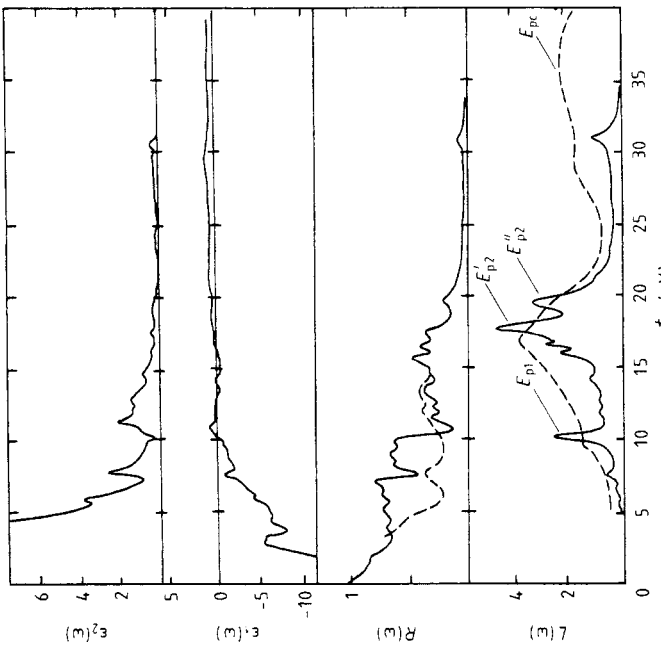

Figure 7. Optical properties of yttrium: full curves, calculations (hcc lattice); dotted curves, measurements (from Weaver and Olson 1977) ($E \perp C$); broken curves, measurements of $L(\omega)$ (from Lynch and Swan 1968) and $R(\omega)$ (from Weaver and Lynch 1973) (arbitrary units).

Figure 8. Optical properties of zirconium: full curves, calculations (hcc lattice); broken curves, measurements of $R(\omega)$ (from Vilesov *et al* 1967) and $L(\omega)$ (from Lynch and Swan 1968) (arbitrary units).

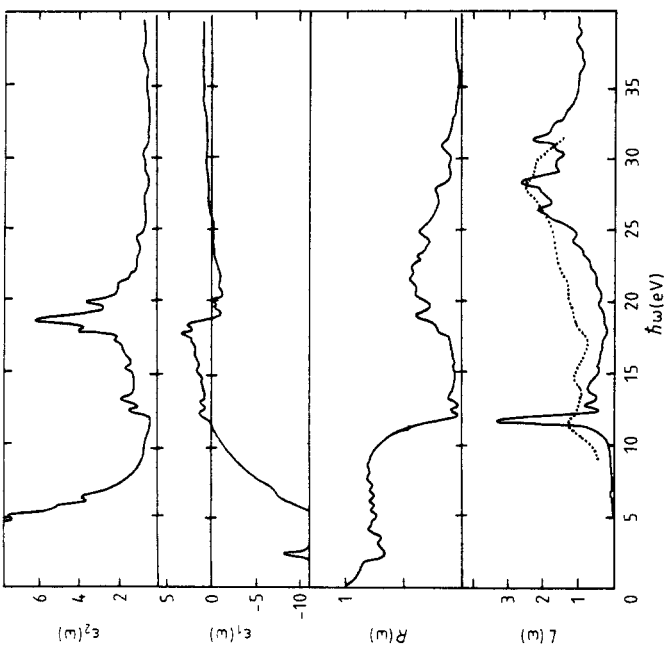

Figure 9. Optical properties of technetium: full curves, calculations (FCC lattice); dotted curve, measurements of $L(\omega)$ (from Zharnikov and Rashkeev 1984) (arbitrary units).

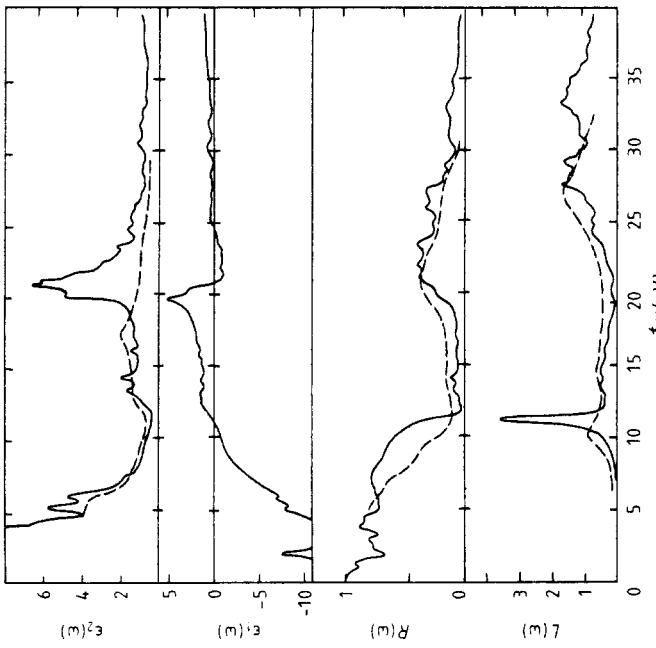

Figure 10. Optical properties of ruthenium: full curves, calculations (FCC lattice); broken curves, measurements (from Gluskin *et al* 1983) (arbitrary units).

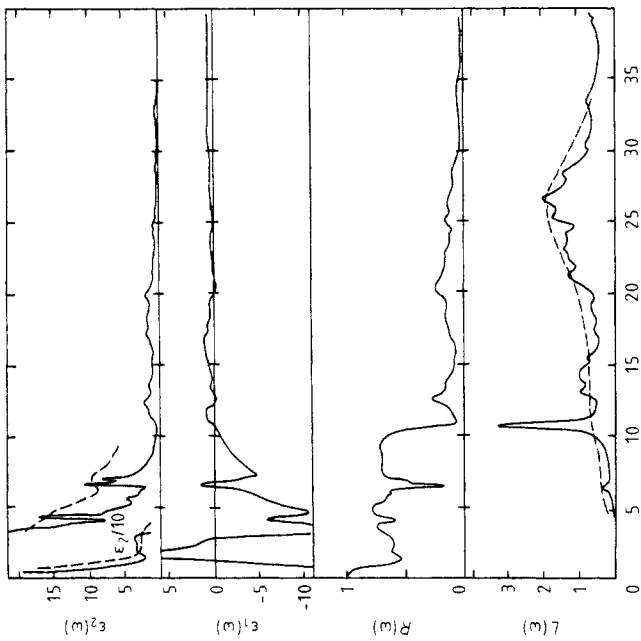

Figure 11. Optical properties of vanadium: full curves, calculations; broken curves, measurements of $\varepsilon_2(\omega)$ (from Weaver *et al* 1974), $R(\omega)$ (from Vilesov *et al* 1967) and $L(\omega)$ (from Szalkowski *et al* 1974); dotted curve, measurements of $L(\omega)$ (from Misell and Atkins 1973) (arbitrary units).

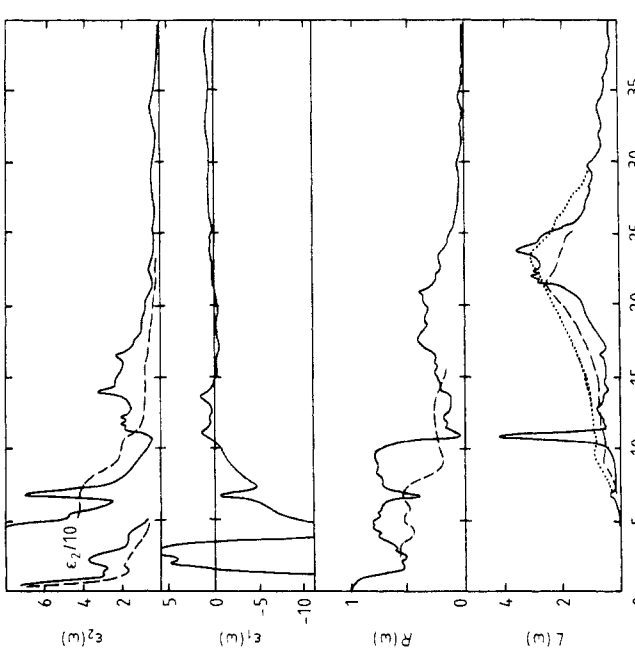

Figure 12. Optical properties of chromium: full curves, calculations; broken curves, measurements of $\varepsilon_2(\omega)$ (from Nestell and Christy 1980) and $L(\omega)$ (from Misell and Atkins 1973) (arbitrary units).

caused by the inadequacy of the LDA or by the non-MT effects, but it should be noted that the available experimental data in this case require verification.

The optical properties of the noble metals Cu and Ag agree very well with experiment (figures 13 and 14). For Cu the calculated optical conductivity $\sigma(\omega) = \omega\varepsilon_2(\omega)/4\pi$ reproduces all the main features of the experimental curve of Beaglehole *et al* (1979) correctly: a sharp increase at $\hbar\omega = 2.1$ eV due to the appearance of the interband transition to the Fermi level; quite a sharp decrease at $\hbar\omega = 6$ eV which is close to the separation between the bottom of the d band and E_F; and a second increase at $\hbar\omega = 15$ eV due to the intensive d–p transitions. A similar situation takes place in Ag. All the main features of $R(\omega)$ and $L(\omega)$ coincide with the experimental ones, and the magnitude of the calculated $\varepsilon_2(\omega)$ also coincides with experiment. It is interesting that the position and even the very existence of the low-energy peak of $L(\omega)$ in Ag ($\hbar\omega = 3.8$ eV), well reproduced in our calculation, are extremely sensitive to the accuracy of $\varepsilon_2(\omega)$. For instance, reducing $\bar{\omega}_p^2$ by only 30% leads to the complete disappearance of the peak, leaving only a small increase of $L(\omega)$. Such good agreement suggests that in the noble metals the LDA Kohn–Sham band structure, particularly the position of the d band, does not differ considerably from the actual one.

Zn and Cd, which follow Cu and Ag in the Periodic Table, share some of their features. In Cd the 4d band lies 2 eV lower relative to the Fermi level than the 3d band in Zn (the corresponding thresholds are 13 eV and 11 eV). The results are the same as in the noble metals: in Cd a well defined peak arises in $L(\omega)$ due to the plasma oscillation of sp electrons; in Zn, instead, a sharp increase of $L(\omega)$ takes place, resembling the shape of $L(\omega)$ in Cu. The agreement of $L(\omega)$ with experiment is reasonable (figures 15 and 16), but the comparison of $R(\omega)$ with the measurements is meaningless, because in fact these metals are hexagonal.

Now, having such a large body of calculational results which generally agree well with experiment, we can analyse the trends and extract from the band structure the properties responsible for the main features of the optical spectra. The following groups of optical transitions are peculiar to transition metals: (i) intraband transitions ($\hbar\omega \leqslant 0.5$ eV); (ii) d–d interband transitions ($0.5 \leqslant \hbar\omega \leqslant 5$–$10$ eV); (iii) d–p transitions ($\hbar\omega \sim 10$–20 eV)—we include in this group the transitions from the partially occupied d bands into the bottom states of the unoccupied hybridised p–f bands; (iv) d–f transitions ($\hbar\omega \sim 20$–50 eV), i.e. the transitions into the top states of the p–f bands. Figure 17 shows the variation of the corresponding oscillator strengths along the 4d series. Unlike in the simple metals, the intraband contribution does not dominate here. The interband d–d contribution is 3–4 times greater. There are comparatively few interband transitions at $\hbar\omega \leqslant 1$ eV, hence the deep minimum in $R(\omega)$ at $0.5 \leqslant \hbar\omega \leqslant 1$ eV. The total d–d oscillator strength (including both intraband and interband d–d transitions) varies along the 4d series in a regular manner: it is small in the early 4d metals, where there are few occupied states, and in the late ones, where there are few unoccupied states, and it increases smoothly to the middle of the series. The d–p transitions are well separated from the d–d ones. Their total oscillator strength is nearly proportional to the number of d electrons (figure 17). This group of transitions at energies $\hbar\omega \sim 20$ eV gradually transforms into the d–f transitions, which turn out to be stronger in the late transition metals (Ru, Rh, Pd).

This discussion is directly applicable to $\varepsilon_2(\omega)$ in the metals under consideration. This defines, in turn, the real part $\varepsilon_1(\omega)$. At $\hbar\omega \leqslant \hbar\gamma \sim 0.1$ eV $\varepsilon_1(\omega)$ is determined from

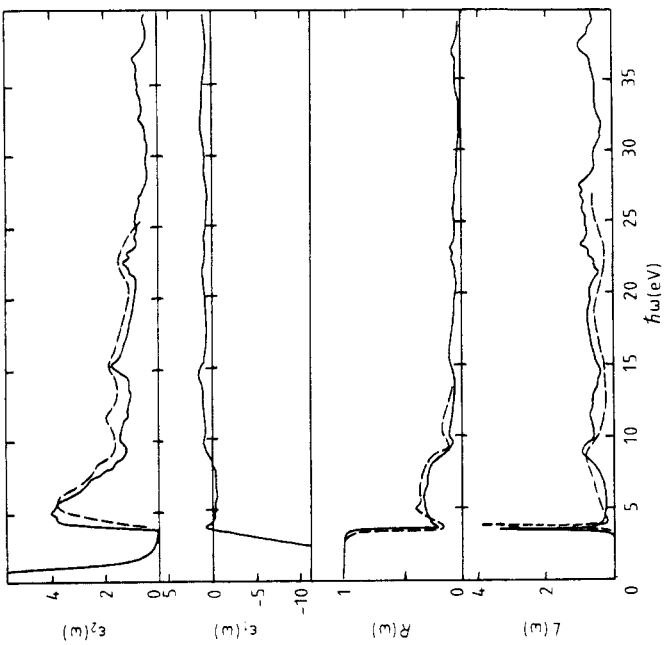

Figure 14. Optical properties of silver: full curves, calculations; broken curves, measurements of $\varepsilon_2(\omega)$ (from Daniels 1969), $R(\omega)$ (from Irani *et al* 1971) and $L(\omega)$ (from Ehrenreich and Philipp 1962) (arbitrary units).

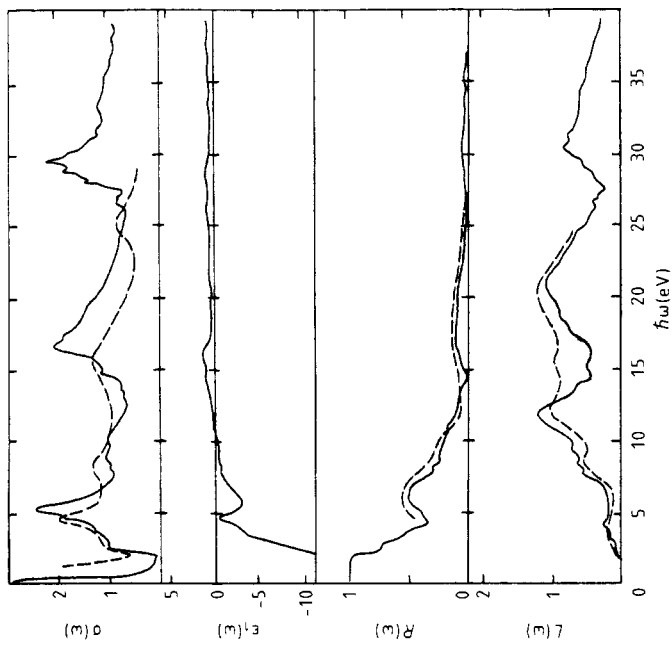

Figure 13. Optical properties of copper: full curves, calculations; broken curves, measurements of $\sigma(\omega)$ (from Beaglehole *et al* 1979), $R(\omega)$ (from Ehrenreich and Philipp 1962) and $L(\omega)$ (from Kubo *et al* 1976) (arbitrary units).

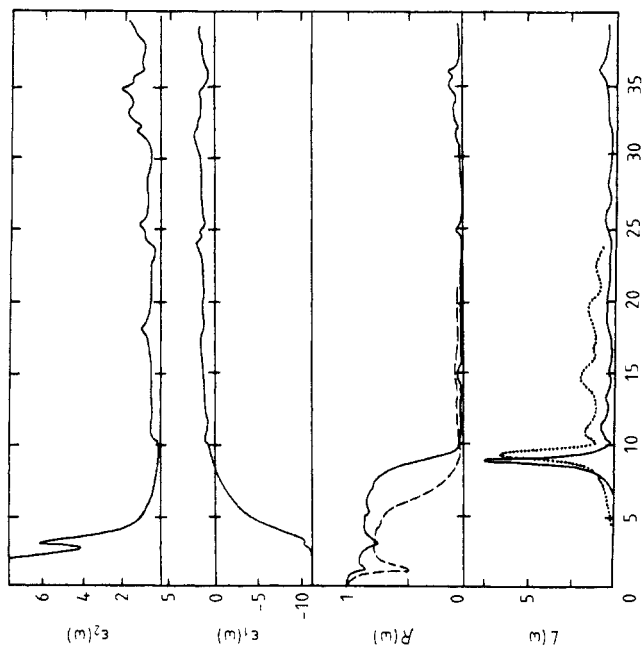

Figure 16. Optical properties of cadmium: full curves, calculations (HCC lattice); broken curve, measurements of $R(\omega)$ (from Bartlett *et al* 1971); dotted curve, measurements of $L(\omega)$ (from Gorobchenko *et al* 1985) (arbitrary units).

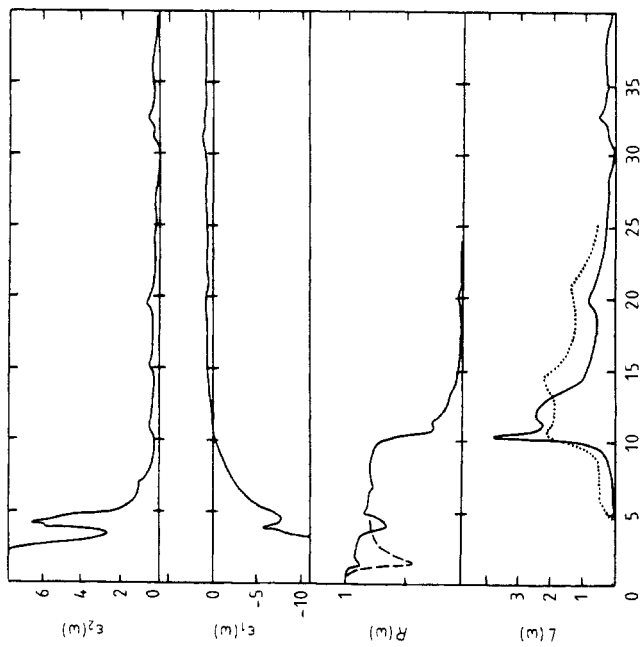

Figure 15. Optical properties of zinc: full curves, calculations (HCC lattice); broken curve, measurements of $R(\omega)$ (from Weaver *et al* 1972) ($\boldsymbol{E} \perp \boldsymbol{c}$); dotted curve, measurements of $L(\omega)$ (from Gorobchenko *et al* 1985) (arbitrary units).

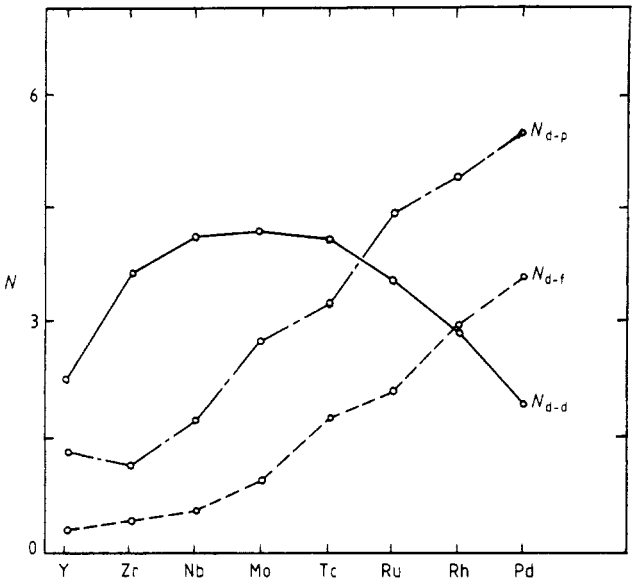

Figure 17. Oscillator strengths of the d–d, d–p and d–f transitions in the 4d metals.

the intraband Drude formula (5):

$$\varepsilon_1(\omega) \approx 1 - \frac{\tilde{\omega}_p^2}{\omega^2 + \gamma^2} < 0.$$

For the (localised in energy) d–d interband transition we add the positive contribution at 1–5 eV and the negative one at 5–10 eV (this may be easily understood using the model $\varepsilon_2(\omega) \sim \delta(\hbar\omega - E_{d-d})$. In the middle 4d metals Mo and Nb, as well as in the 3d metals V and Co, where the d–d transitions are very strong, $\varepsilon_1(\omega)$ in this region increases to zero and even to positive values. $\varepsilon_2(\omega)$ is not small in this region and this prevents the appearance of a plasmon. However, it does affect $R(\omega)$. Indeed, it can be shown that when $\varepsilon_2(\omega) \gg 1$, $(1 - R(\omega)) \approx 4|\varepsilon(\omega)|^{-1/2}$ and the sharp decrease in magnitude of $\varepsilon_1(\omega)$ gives rise to a minimum in $R(\omega)$. Such minima are clearly seen in the corresponding figures.

An analogous but much stronger effect takes place at higher energies. Just before the beginning of the d–p transitions, a positive contribution to $\varepsilon_1(\omega)$ is added to the Drude part and $\varepsilon_1(\omega)$ goes through zero. $\varepsilon_2(\omega)$ is quite small here due to the gap between the d–d and d–p transitions and a sharp strong plasmon peak appears. The position E_{p1} of this plasmon is fixed in the above mentioned gap and does not vary much from one metal to another. In particular it does not correlate with the number of valence electrons. Near E_{p1}, $R(\omega)$ has a minimum analogous to the plasmon reflectivity edge in simple metals. In this region $\varepsilon_2(\omega) \ll 1$, and $R(\omega) \approx 1$ when $\varepsilon_1(\omega) < 0$ and decreases at $\varepsilon_1(\omega) > 0$. Thus a dip in $R(\omega)$ occurs when ε_1 goes through zero.

In the early and middle transition metals the d–p and d–f transitions are separated by a region of low conductivity. Just before this region $\varepsilon_1(\omega)$ decreases again to negative values (this is called 'anomal dispersion' in dielectrics optics) and then

returns to positive values, approaching unity at $\omega \rightarrow \infty$. This third zero of $\varepsilon_1(\omega)$ occurs in the low-conductivity region and gives rise to a second plasmon, more smoothed than the first one, with an energy E_{p2} (hence another decrease of reflectivity). The fact that E_{p2} falls between the d–p and d–f transitions is not accidental: according to the effective number of electrons involved in this plasmon it should be found at a lower energy, but it is 'pushed up' by the strong d–p transitions. In fact the coincidence of E_{p2} with the classical plasma energy $\hbar\omega_p$ calculated with all the valence electrons is accidental. This question is discussed in detail by Mazin *et al* (1986).

In the late transition metals (Ru, Rh, Rd) the regions of the d–p and d–f transitions are contiguous; therefore $\varepsilon_1(\omega)$ decreases very slowly and does not change sign at $\hbar\omega > E_{p1}$. The high-energy EELS in these metals have a few very smoothed features defined by the structure of the p–f bands. The strong plasmon E_{p2} is non-existent here and the features of $R(\omega)$ show no general trends.

4. Conclusions

We have described a method of calculating optical properties and applied it to 15 metals. In the energy range where the LMTO method allows us to obtain the band structure and the matrix elements accurately enough, the agreement with experiment is very good. Thus there is a good opportunity to use these calculations for a detailed analysis of the optical properties of metals and the different factors which essentially determine them. In fact such a detailed analysis of the infrared optics of transition metals has been published by us elsewhere (Rashkeev *et al* 1985), where we have shown that the intraband optics at very low frequencies ($\hbar\omega \leqslant 0.7$ eV) is much richer than had been thought. Also we have performed a detailed comparative study of the electron energy loss spectra in transition metals (Mazin *et al* 1986), in which it was shown that the underlying physics is very complicated in comparison with simple metals and cannot be understood in terms of the usual 'plasmon excitation' of Pines.

References

Alouani M and Khan M A 1986 *J. Physique* **47** 453–60
Andersen O K 1975 *Phys. Rev.* B **12** 3060–3
Bartlett R J, Lynch D W and Rosei R 1971 *Phys. Rev.* B **3** 4074–81
Beaglehole D, De Crescenti M, Theye M L and Vuye G 1979 *Phys. Rev.* B **19** 6306–17
Daniels J 1969 *Z. Phys.* **227** 234–51
De Sorbo W 1963 *Phys. Rev.* **132** 107–20
Ehrenreich H and Cohen M H 1959 *Phys. Rev.* **115** 786–92
Ehrenreich H and Philipp H K 1962 *Phys. Rev.* **128** 1622–8
Gluskin E S, Druzhinin A V, Kirillova M M, Kochubei V I and Nomerovannaya L V 1983 *Opt. Spektrosk.* **55** 891–7
Gorobchenko V D, Zharnikov M V, Maksimov E G and Rashkeev S N 1985 *Zh. Eksp. Teor. Fiz.* **88** 677–91
Irani G B, Huen T and Wooten E 1971 *Phys. Rev.* B **3** 2385–94
Kubo Y, Wakoh S and Yamashita J 1976 *J. Phys. Soc. Japan* **41** 1556–62
Lynch M J and Swan J B 1968 *Aust. J. Phys.* **21** 811–9
Mayevskii V M, Druzhinin A V, Kirillova M M and Nomerovannaya L V 1981 unpublished (available from Moscow Baltiyskaya 14 VINITI Depon. Rukop. N5151-81)
Mazin I I, Maksimov E G, Rashkeev S N and Uspenskii Yu A 1986 *Zh. Eksp. Teor. Fiz.* **90** 1092–110
Mazin I I, Savitskii E M and Uspenskii Yu A 1984 *J. Phys. F: Met. Phys.* **14** 167–78

Misell D L and Atkins A J 1973 *Phil. Mag.* **27** 95–104
Moruzzi V L, Janak J F and Williams A R 1979 *Calculated Electronic Properties of Metals* (New York: Pergamon)
Motulevich G P 1969 *Usp. Fiz. Nauk* **97** 211–335
Nestell J E and Christy R W 1980 *Phys. Rev.* B **21** 3173–9
Pierce D T and Spicer W E 1973 *Phys. Status Solidi* b **60** 689–95
Pines D 1963 *Elementary Excitations in Solids* (New York: Benjamin)
Rashkeev S N and Halilov S F 1987 *Metallofizika* **9** 15–20
Rashkeev S N, Uspenskii Yu A and Mazin I I 1985 *Zh. Eksp. Teor. Fiz.* **88** 1689–98
Runge E and Gross E K V 1984 *Phys. Rev. Lett.* **52** 997–1000
Seignac S and Robin S 1970 *C. R. Acad. Sci. Paris* B **271** 919–24
Shiles E, Sasaki T, Inokuti M and Smith D Y 1980 *Phys. Rev.* B **22** 1612–26
Singhal S P 1976 *Phys. Rev.* B **14** 2352–61
Smith D Y and Shiles E 1978 *Phys. Rev.* B **17** 4689–94
Sturm K 1982 *Adv. Phys.* **31** 1–83
Szalkowski F J, Bertrand P A and Somorjay G A 1974 *Phys. Rev.* B **9** 3369–78
Tups H and Syassen K 1984 *J. Phys. F: Met. Phys.* **14** 2753–69
Uspenskii Yu A, Maksimov E G, Rashkeev S N and Mazin I I 1983 *Z. Phys.* B **53** 263–70
Vehse R C, Arakawa E T and Williams M W 1970 *Phys. Rev.* B **1** 517–26
Vilesov F I, Zagrubskii A A and Kirillova M M 1967 *Opt. Specktrosk.* **23** 153–62
Weaver J H 1973 *Phys. Rev.* B **11** 1416–24
Weaver J H and Lynch D W 1973 *Phys. Rev.* B **7** 4737–42
Weaver J H, Lynch D W and Olson C G 1973 *Phys. Rev.* B **7** 4311–9
—— 1974 *Phys. Rev.* B **10** 501–16
Weaver J H, Lynch D W and Rosei R 1972 *Phys. Rev.* B **5** 2829–32
Weaver J H and Olson C G 1977 *Phys. Rev.* B **15** 590–4
Wooten F 1972 *Optical Properties of Solids* (New York: Academic)
Zangwill A and Soven P 1980 *Phys. Rev.* A **21** 1561–77
Zharnikov M V and Rashkeev S N 1984 *Fiz. Tverd. Tela* **26** 3385–9